J. Mol. Biol. (1994) **238**, 437–444

Ultrafast Measurements of Geminate Recombination of NO with Site-specific Mutants of Human Myoglobin

J. W. Petrich[1]†, J.-C. Lambry[1], Sriram Balasubramanian[2] David G. Lambright[2], Steven G. Boxer[2]‡ and J. L. Martin[1]‡

[1]*Laboratoire d'Optique Applique, Ecole Polytechnique ENSTA, INSERM U275, 91128 Palaiseau Cedex, France*

[2]*Department of Chemistry, Stanford University Stanford, CA 94305-5080, U.S.A.*

Flash photolysis studies of NO recombination to heme proteins offer a direct probe of protein structural changes on the tens of picoseconds timescale where they can be compared with molecular dynamics simulations. The geminate recombination of NO to site-specific mutants of human myoglobin (Mb) was studied following photodissociation of the MbNO form. Single amino acid changes were introduced at positions Val68, His64, Lys45 and Asp60 because motions of residues at these positions are generally regarded as important for the mechanism of ligand binding. In sharp contrast to the properties of simple porphyrin–NO complexes, the rebinding kinetics are found to be non-exponential for all mutants, even in aqueous solution at 298 K. The Val68 and His64 mutants substantially affect the NO rebinding rates but, surprisingly, so do changes on the protein surface that are further away from the iron. These changes in kinetics occur on a tens of picoseconds timescale, and therefore there is either a fast communication between protein residues over quite long distances or there are subtle differences in protein structure that exert great control over the reaction dynamics. Various models for the rebinding kinetics are evaluated. A model-free approach to data analysis using the maximum entropy method is found to be most useful. This analysis shows that the rate distributions are very different for the mutants, but are generally bimodal.

Keywords: human myoglobin; mutagenesis; kinetics; structure–function relationships; picosecond timescale

1. Introduction

Nitric oxide is found in a wide range of biological systems and exhibits diverse and important functions (Snyder & Bredt, 1992; Traylor & Sharma, 1992). NO can be used as a probe of protein dynamics in heme proteins, because the kinetics of recombination of NO following flash photolysis occurs on a picosecond timescale and can be compared directly with molecular dynamics simulations. Following photodissociation, a series of motions are initiated, at first centering around the heme Fe atom, and then becoming more global and continuing on the nanosecond timescale (Petrich *et al.*, 1991; Xie & Simon, 1991; Genberg *et al.*, 1991; Elber & Karplus, 1990). The barrier to NO rebinding has only a small contribution from electronic factors (Petrich *et al.*, 1988; Cornelius *et al.*, 1983), unlike carbon monoxide rebinding, which has been much more extensively studied. As a result, the NO rebinding kinetics are expected to depend primarily on the protein response (Case & Karplus, 1979). Rather little is known about the molecular details of these motions and how they are governed by amino acid residues that make up the heme binding pocket.

The rebinding of NO to site-specific mutants of myoglobin (Mb§) offers an approach to probe more deeply into these fast timescale protein dynamics. The X-ray crystal structures of many Mbs and their mutants are known (Kendrew *et al.*, 1960; Kuriyan

† Present address: Department of Chemistry, Iowa State University, Ames, IA 50011, U.S.A.

‡ Author to whom all correspondence should be addressed.

§ Abbreviations used: Mb, myoglobin; MbCO, carbonmonoxy myoglobin; MbNO, nitrosyl myoglobin; Hb, hemoglobin; WT, wild-type; SW, sperm whale; NMR, nuclear magnetic resonance; IR, infrared; MEM, maximum entropy method.

0022-2836/94/180437 08 $08.00/0

et al., 1986; Hubbard *et al.*, 1990; Smerdon *et al.*, 1991) and the structural perturbation can be kept small and pin-pointed to a fair degree of accuracy. The choice of mutants in this study derives from earlier theoretical (Case & Karplus, 1979) and experimental work (Ringe *et al.*, 1984; Lecomte & La Mar, 1985; Kuriyan *et al.*, 1986) regarding the motions of protein residues involved in ligand binding to Mbs. It has been proposed that the highly conserved distal residues Val68 and His64 are important in the final binding step at the heme iron, at least for CO and O_2 recombination (Case & Karplus, 1979). A detailed analysis of the CO recombination to human Mb mutants at these positions near room temperature is presented elsewhere (Lambright *et al.*, 1989, 1991; Balasubramanian *et al.*, 1993*b*). These kinetics sample the timescale from tens of nanoseconds to milliseconds. Substantial effects are observed, especially for the geminate phase of the rebinding. It is not obvious that these distal residues should also significantly influence the ligand binding dynamics on the timescale of a few tens of picoseconds, where simulations suggest that the functionally important motions are largely localized to the iron atom and the bound proximal histidine residue (Petrich *et al.*, 1991). Furthermore, surface residues, such as those at positions 45 and 60, which are believed to be important in the gating of ligands in and out of the protein (Case & Karplus, 1979; Ringe *et al.*, 1984; Lecomte & La Mar; 1985), might not be expected to affect ultrafast processes within the heme binding pocket. We show in this study that significant changes in the NO rebinding kinetics are obtained not only with changes in the immediate vicinity of the iron, but also from several that are much further away.

2. Experimental Methods

(a) *Sample preparation*

The human Mb mutants used in this study are all based on the site-specific mutant C110A of human Mb, hereafter designated WT. The preparation and purification of these mutants has been described (Lambright *et al.*, 1989; Varadarajan *et al.*, 1989). The preparation of the MbNO samples from the met forms has also been described (Petrich *et al.*, 1987). The absorption spectra of the NO forms of WT human Mb and its mutants used in this study are virtually identical with that of sperm whale Mb, as has been noted for the CO-bound species (Lambright *et al.*, 1989; Balasubramanian *et al.*, 1993*b*).

(b) *Photolysis system*

The laser apparatus and data collection have been described in detail in an earlier publication (Petrich *et al.*, 1988). The samples were excited at 574 nm, and the kinetics were probed at 442 nm. Because NO recombination is observed to occur on a timescale of tens of picoseconds and the laser pulsewidth is 150 fs, it is not necessary to include the effects of the pulse in the subsequent analysis. It has been established that the optical changes at 442 nm are due to the kinetics of NO religation and not to transient absorption of heme-excited states, which absorb at much longer wavelengths and are very short-lived (Petrich *et al.*, 1988). The conditions of photolysis are the same as those described earlier (Petrich *et al.*, 1991). It has been checked that increasing by a factor of 2 or 3 the percentage of photolyzed NO molecules, does not affect the measured rates of rebinding. The delay line used in the experiment permitted examination of events to 360 ps. By this time the recombination is more than 85% complete for all the proteins examined in this study.

3. Results and Data Analysis

The kinetics of NO recombination to WT human Mb are compared with those of the mutants K45R and D60E at room temperature in Figure 1. Similarly, the recombination curve for WT is compared with those for V68A, V68N and H64Q in Figure 2 and with K45A and K45Q in Figure 3. It is apparent that the kinetics are very different when the residue at position 68 is changed, while they are more similar for the mutations at position 45, with the exception of K45R. The recombination is virtually complete within the experimental time window for V68A and is more than 85% complete for the other proteins.

The kinetics are non-exponential for all the proteins studied. As a starting point, the data have been fit using least-squares minimization (Press *et al.*, 1989) to two functions used earlier to fit the kinetics of NO recombination to sperm whale Mb and human hemoglobin (Petrich *et al.*, 1991).

Model I, which is a sum of exponentials:

$$\Delta A(t) = A_1 \exp(-k_1 t) + A_2 \exp(-k_2 t) + \text{baseline} \quad (1)$$

and model II, which utilizes a time-dependent barrier height:

$$\Delta A(t) = \exp\left[-\int_0^t k(t)\,\mathrm{d}t\right]. \quad (2)$$

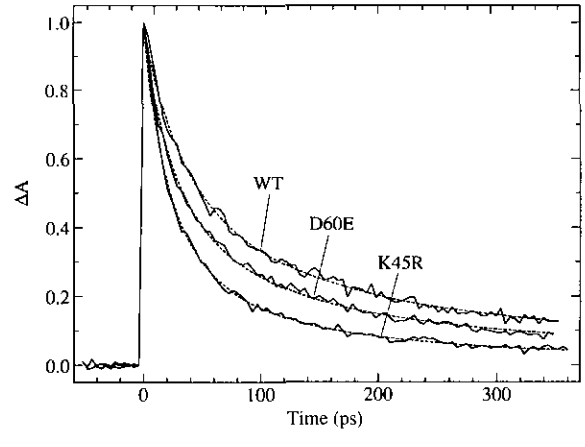

Figure 1. NO recombination at 298 K following photodissociation of NO-bound human myoglobin WT and the surface mutants D60E and K45R. The continuous lines are the data, and the broken lines are fits to model I (see the text). The parameters from fits such as these for all the proteins in this study are listed in Table 1. The data are shown as induced absorption and the curves in this and the 2 following Figures have been normalized to 1 at the maximum ΔA, which is taken to be $t=0$.

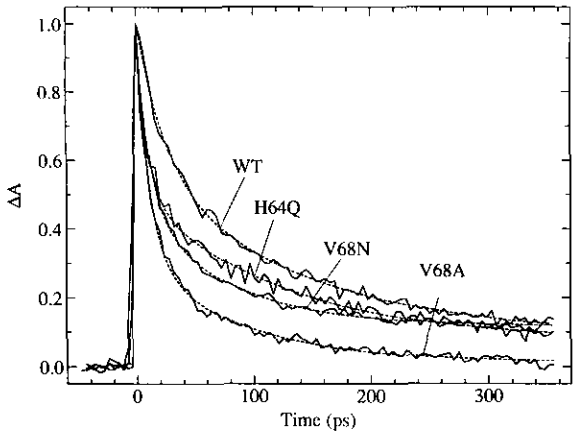

Figure 2. NO recombination kinetics for mutations in the heme pocket at positions 64 and 68 (His and Val respectively in WT, which is shown for comparison). The continuous lines are the data, and the broken lines are fits to model II (see the text for discussion). The parameters from the fits are listed in Table 2.

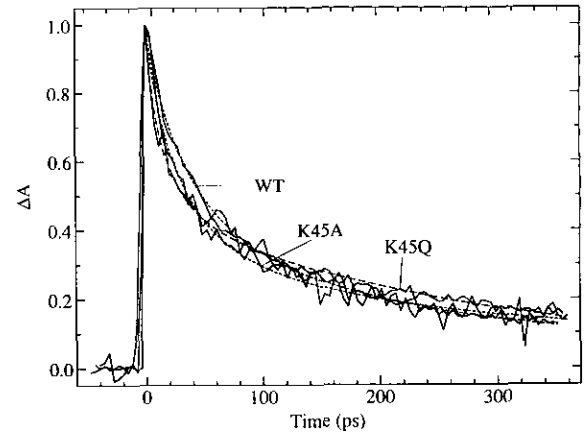

Figure 3. NO recombination kinetics for WT and 2 mutations at position 45, which is a solvent-exposed surface position (Ringe *et al.*, 1984; Kuriyan *et al.*, 1986; Hubbard *et al.*, 1990). The continuous lines are the data and the broken lines are fits to the time-dependent barrier model, model II (see the text). The parameters from these fits are also listed in Table 2.

The barrier decay rate $k(t)$ in model II is given by:

$$k(t) = A \exp[-E(t)/RT], \quad (3)$$

and the time dependence of the barrier height is given by:

$$E(t) = (E_0 - E_{eq}) \exp(-k_{bar} t) + E_{eq}, \quad (4)$$

where k_{bar} is the rate constant that determines the evolution of the barrier from its initial height E_0 to its equilibrium value E_{eq}. The parameters from these fits are shown in Tables 1 and 2. The reduced χ^2 values from these fits are very similar if an adjustable baseline is allowed for model I, and we

Table 1

Fits of NO recombination data to model I

Protein	Amplitude A_1	Rate k_1 $\times 10^{10}s^{-1}$	Amplitude A_2	Rate k_2 $\times 10^{9}s^{-1}$	Baseline†
WT	0·44	4·08	0·49	7·14	0·08
D60E	0·45	5·98	0·49	9·05	0·07
K45R	0·58	5·94	0·39	11·5	0·04
K45A	0·49	5·66	0·42	8·85	0·12
K45Q	0·41	9·21	0·44	7·62	0·13
H64Q	0·48	11·2	0·43	8·20	0·07
V68A	0·65	8·98	0·32	11·9	0·01
V68N	0·51	9·17	0·36	13·5	0·12

Parameters are defined in the text under model I. The errors in the parameters are ±6% at the 1σ level.

†Amplitudes have been normalized so that $A_1 + A_2 + \text{baseline} = 1$.

Table 2

Fits of NO recombination data to Model II

Protein	Arrhenius prefactor A $\times 10^{10}s^{-1}$	Barrier heights: Initial E_0 (kJ mol^{-1})	Barrier heights: Final E_{eq} (kJ mol^{-1})	Barrier relaxation rate k_{bar} $\times 10^{10}s^{-1}$
D60E	3·10	0·002	4·93	1·43
K45R	3·94	0·066	5·87	0·96
K45A	2·77	0·001	6·54	0·95
K45Q	4·51	0·015	6·59	2·46
H64Q	6·48	0·003	6·64	3·12
V68A	7·55	0·001	5·57	2·4
V68N	5·25	0·001	8·13	1·3

Parameters are defined in the text under model II. The errors at the 1σ level are ±8% in the prefactors, ±11% in the barrier heights and ±15% in the barrier relaxation rates.

are therefore unable to decide between these models from the quality of the fits alone. To check if a residual baseline offset is due to ligands that escape from the pocket and recombine *via* a bimolecular process, the NO recombination kinetics for the three proteins that show the largest residual baseline at 400 ps (WT, K45A and V68N) were examined using a transient absorbance setup with 8 ns excitation pulses (Lambright *et al.*, 1991). Within the noise level of the experiment (0·5% of the initial ΔA), no evidence was found for NO recombination from 30 ns to several milliseconds. We conclude that all the NO has rebound within a few nanoseconds in all the proteins, consistent with what has been assumed in previous studies. As will be shown shortly, the rebinding rates are distributed; therefore, the baseline offset likely represents the slow rebinding part of the population.

In order to make further progress, other methods are needed to obtain further information about the system. One approach is to perform molecular dynamics simulations and compare them with the experimental results (Petrich *et al.*, 1991). A simple and direct approach is to obtain the underlying distribution of rates without the assumption of any model. One can then examine more specific models in the light of the conclusions from the model-free analysis. In earlier work on CO rebinding (Lambright *et al.*, 1993) it has been found useful to obtain the rate distributions from the kinetic curves by using the maximum entropy method (MEM) (Jaynes, 1986; Skilling & Gull, 1985; Skilling, 1988). In this approach, an entropy function is maximized subject to the constraint that the reduced χ^2 be near 1, and a distribution of probabilities of the underlying rate components is obtained (Skilling, 1988). It must be emphasized that the resulting distribution is the most probable, but not unique, rate distribution that describes the observed kinetics. The detailed results of such an analysis are shown for human WT MbNO in Figure 4. The top panel of Figure 4A shows a comparison of this model with the data, and the bottom panel shows the residuals. The distribution of rates is shown in Figure 4B. In order to refrain from overfitting the data, it is necessary to obtain a good estimate of the errors in the data. This has been done by fitting the data to a double exponential plus baseline and adjusting the errors so that the reduced χ^2 is 1†. The parameters from this fit are shown as the diamond-tipped spikes in Figure 4B. The heights of the spikes represent the amplitudes associated with each exponential rate. Also shown are the parameters from a double exponential fit with the baseline fixed at zero (circle-tipped spikes). It is evident that the rate constants from the fits including a baseline better match the peaks of the distribution obtained by MEM. This is interesting, but not surprising, as the exponential fits are only an approximation to the true distribution of rates; the broader the distribution, the larger the number of parameters needed to fit it. For example, for V68A, where the recombination is complete within 400 ps, three exponentials are required for a satisfactory fit. The baseline seen in the slower rebinding mutants presumably represents the third exponential.

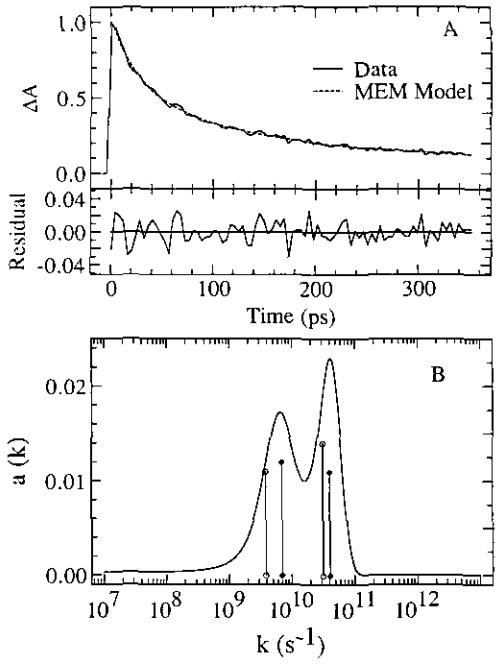

Figure 4. A, NO recombination data for human WT Mb is shown in the upper panel (continuous lines) together with the fit from the model function obtained from the maximum entropy method (MEM) analysis. Details are discussed in the text. The bottom panel shows the residuals from this fit on an expanded scale. B, The resulting distribution of rate constants for NO recombination to WT obtained from the MEM analysis above. The vertical lines represent the best fit rate constants from a bi-exponential fit, with (diamonds) and without (circles) a baseline. The amplitudes of the lines are scaled down by 40 for viewing purposes from the normalized amplitudes obtained from the fits. a(k), sum of amplitudes.

The distributions of rates obtained from MEM analysis are shown in Figure 5. The rate distribution of WT is compared with those of D60E and K45R in Figure 5A, and with those of V68A and V68N in Figure 5B. Figure 5C shows the effect of changing the distal residue from histidine to glutamine, as found in elephant Mb. Note that the sum of the amplitudes $a(k)$ in all the Figures has been normalized to 1.

† In order to be certain that the data are still not overfit, this estimate was verified by other means.

(1) The MEM fit was continued until the data were fit to flatness; the χ^2 at this point was noted, and it was verified that the χ^2 level in the MEM fits shown was at least 10% above this level.

(2) An autocorrelation function of the form $A = \Sigma(y_i y_{i-1})/\Sigma y_i^2$ was constructed; a number of datasets containing different levels of Gaussian noise were generated. Using the autocorrelation of these as a lower limit, it was verified that the autocorrelation of the residuals from the MEM fits were all above this limit.

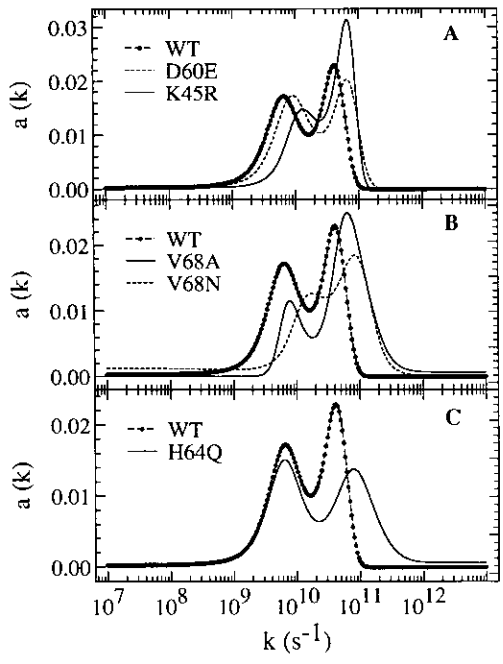

Figure 5. A. Rate distributions for NO recombination obtained from the MEM analysis are shown for the proteins from Figure 1. B, Rate distributions for NO recombination obtained from the MEM analysis are compared for WT and the valine 68 mutants. C, Rate distributions for NO recombination from the MEM analysis for different residues at the distal position: WT (His) and H64Q (Gln). Note the increased width and faster recombination for H64Q as compared with WT.

4. Discussion

Previous analyses of NO recombination have tended to be model-specific, and there seems to be little agreement on the correct model. Most models have been variations on a sequential scheme with at least two intermediates, each of which could have a number of substates (Jongeward *et al.*, 1986, 1988; Gibson *et al.*, 1986). An active area of research is to determine the relative effects of the proximal and distal parts of the heme pocket on the rebinding kinetics. One model with two states and a rebinding barrier that increases with time has been considered (Petrich *et al.*, 1991). In this model, immediately upon ligand dissociation, the proximal side, especially variations in the iron-heme coordinate, is most likely to control ligand rebinding. On the other hand, Ikeda-Saito *et al.* (1993) and Li *et al.* (1993) have considered the effects of diffusion in the distal side of the heme pocket.

The fits in Table 2 show that consideration of only the proximal side can fit all the data for a variety of mutants. However, since the applicability of such specific models still awaits rigorous experimental scrutiny, the approach we have chosen here is to analyze the data using a method that is relatively free of assumptions about the nature of the reaction, and then briefly consider the results in the light of previous work. The model-free MEM analysis leads to a number of general conclusions.

The NO rebinding kinetics are influenced by every mutation investigated in this paper. Most of the mutations are on the distal side, and some, for example D60E, are quite far from the iron. It is unlikely that an adequate understanding of the relative roles, or of the interplay, of the proximal and the distal parts of the heme pocket will be attained by structural studies alone, as some of the changes are probably too small to be observed by conventional crystallographic methods. For instance, the structure of the mutant K45R in the met form has been determined by X-ray crystallography (Hubbard *et al.*, 1990), and it is virtually identical with that of SW Mb, yet the NO kinetics are significantly different (Figure 1 (K45R) and Figure 3b of Petrich *et al.*, 1991 (SW Mb); also see Table 1). Infrared spectroscopy of the ligand-bound form is exquisitely sensitive to the details for ligand bonding and has been recently used for understanding the reactions of the CO-bound forms of Mb and its mutants (Balasubramanian *et al.*, 1993*a*; Adachi *et al.*, 1992). However, there has been very little work on the infrared spectroscopy of the NO form, due to difficulties of high solvent and protein backbone amide absorbances in the N–O stretch region (1550 to 1700 cm^{-1}) (Maxwell & Caughey, 1976) and the rapid recombination rate.

Spectroscopic studies have also contributed evidence of protein relaxations on the picosecond timescale, which has been supported by dynamics simulations (Petrich *et al.*, 1991). Such relaxations might be expected to affect the rates of NO rebinding that we observe. In terms of the rate distributions that are obtained from MEM, a relaxation of the rebinding barrier on the timescale of the early rebinding would be expected to broaden the early-time distribution; conversely, if the barrier at early times did not change appreciably, a narrow width for the early rebinding would be predicted (the limiting case of a singe exponential rate would look like a spike such as those in Figure 4B, with a finite width depending on the signal-to-noise ratio of the data and the grid resolution used for the MEM). Figure 5 shows that there are significant differences in the widths of the early-time distributions: the mutants at the surface (Figure 5A) exhibit the narrowest early-time distribution as measured by the widths of the peak corresponding to the faster rates, while it is broader for the mutants at positions 64 and 68 (Figure 5B and C).

The data in Figures 1 through 3 and the MEM results in the succeeding Figures clearly show that the rebinding is non-exponential for all the mutants and that the resulting distribution of rates is not unimodal. This indicates that functions such as a power law, which is the Laplace transform of a unimodal distribution of rates (see, for e.g. Austin *et al.*, 1975), would be inappropriate even if a reasonable fit were obtained to the kinetic curve. To emphasize this result, it is seen that even H64Q has a bimodal distribution of rates (Figure 5A); this contrasts with earlier reports of single exponential NO rebinding kinetics for elephant Mb, which also

contains glutamine in place of the distal histidine residue (Jongeward *et al.*, 1986, 1988). Furthermore, the kinetics appear to be more distributed than for WT; the slower peak is similar to WT, while the faster peak is significantly broader. This parallels the rebinding of CO to H64Q: the initial rebinding is faster than WT, while the later rebinding is quite similar (Lambright *et al.*, 1993). These results confirm that the substitution of glutamine for histidine at position 64 creates a broader distribution of rates, perhaps due to the greater flexibility of the glutamine side-chain as compared with the imidazole ring of the histidine.

The MEM results for the surface mutants K45R and D60E (Figure 5A) show that both peaks in these mutants are shifted to higher rates than for WT. Thus, the rebinding is faster in both cases; however, the early peak for K45R is much larger than for WT, while that for D60E is somewhat smaller. In the case of K45R, this result, together with the narrow width of the early-time peak indicates that a greater fraction of the rebinding occurs before the protein relaxes appreciably.

Comparatively larger deviations from WT behavior are found for the valine 68 mutants V68A and V68N (Figures 2 and 5B). The observed rebinding kinetics are twofold faster than WT for both mutants (Figure 2 and Table 1); in the MEM distributions (Figure 5B) this is shown by a shift of the peaks to higher rates. While the rebinding in V68A is complete in 360 ps, in V68N there is a very slow rebinding component. Thus, V68N appears to have the largest range of recombination rates in this set of mutants. The shapes of the MEM distributions for the Val68 mutants are also very different from WT; the early-time peak appears to be much broadened relative to WT, suggesting that the protein relaxation is faster. Even then, much of the rebinding still occurs at early times for these mutants (as shown visually by the relative areas of the peaks), particularly for V68A. Support for these interpretations can be found in parallel data for CO rebinding, where a careful analysis of the transient difference spectrum shows a protein relaxation process that is faster in V68A than in WT (Lambright *et al.*, 1993).

Although the MEM analysis provides a useful approach for comparing the properties of mutants that is independent of the exact nature of the underlying processes, it also raises many interesting questions. For example, why do V68A, V68N and H64Q show a large fraction of early rebinding in spite of fast relaxation of the protein? A possible answer can now be obtained by considering a molecular model such as the time-dependent barrier model. From the parameters in Table 2 it is seen that the barrier heights for the recombination are quite small, and that the prefactors for the Val68 and His64 mutants are about threefold larger than WT. This suggests that the early rebinding is determined largely by the prefactor. In confirmation of this, it is seen from the MEM results that the faster peak for each mutant correlates with the value of the prefactor in Table 2. Further, the mutants that have broader MEM distributions at early times also show a faster barrier decay rate, which is a measure of the protein relaxation in this model. Temperature-dependent kinetic studies will be needed to ascertain that NO rebinding in these mutants is, in fact, a prefactor-dominated reaction.

As a final point, we note that the sensitivity of this experiment is shown by the differences in the kinetics for the Lys45 and Asp60 mutants. While these changes are smaller than for the Val68 and His64 mutants, some substantive trends are seen. Figure 1 and Figure 5B show that the rebinding is faster in the order WT < D60E < K45R. As discussed above and reflected in the parameters in Table 2, this is mainly due to the change in the prefactor. One interpretation of this could be that the activation entropy ΔS is less negative in the mutants, i.e. the difference in entropy between the reactants and the transition state is smaller than in WT. However, chemical reaction dynamics on such short timescales is still an active area of research, and it is not clear that such a simple interpretation is necessarily valid. The fact remains that the mutations at positions far away from the iron do affect the kinetics, and this necessitates further consideration of distal effects even on the picosecond timescale.

NO recombination to Mbs from different species has been studied by several groups (Jongeward *et al.*, 1986, 1988; Carver *et al.*, 1991; Ikeda-Saito *et al.*, 1993; Li *et al.*, 1993). As mentioned earlier, NO rebinding to elephant Mb, which has glutamine in the position of the distal histidine residue, was reported to be well fit with a single exponential (Jongeward *et al.*, 1986, 1988), which is clearly not what we observe for the corresponding single mutant in human Mb. The difficulties in understanding the role of a specific residue by comparison of the same protein (Mb) in different species (elephant and human) are likely to be at the origin of this apparent discrepancy. Our result agrees with a study on the corresponding mutant of SW Mb (Carver *et al.*, 1991), in that at least two substates were required to fit the data. However, while the slower rate constants for SWMb H64Q are similar to those of the reference wild-type, which is what we also observe for human Mb H64Q, the faster rate reported by these authors was nearly the same as for native SW MbNO, which is at odds with our result, that H64Q shows much faster recombination at early times. Since the event-time for this process is of the order of 40 ps and the pulsewidth in the study reported by Carver *et al.* (1991) was about 35 ps, the disagreement may be due to the instrumental limitations of the latter study. This may explain why these authors concluded that the V68A mutation did not perturb the fast rebinding.

We have already carried out a thorough investigation of the kinetics of ligand rebinding in the CO form to these mutants (Lambright *et al.*, 1989, 1991; Balasubramanian *et al.*, 1993*b*). As already noted, there are considerable parallels in the trends among

the mutants with the NO rebinding kinetics. For example, we may note the case of the interesting mutant V68N, which also shows both a larger prefactor and a larger rebinding barrier in the CO reaction. In the case of the CO kinetics, the rebinding barrier is much larger, and leads to substantial temperature dependencies for this reaction. There is considerable evidence that the kinetics can be related to the populations of the different bound CO conformers seen in the infrared spectrum (Balasubramanian *et al.*, 1993*a*; Tian *et al.*, 1992). The similarity between the CO and the NO kinetics would suggest, therefore, that the structure of the initial photodissociated state is similar in both cases, and it is the dynamics of the subsequent relaxation that governs the rebinding kinetics. As mentioned earlier, the infrared stretch region of bound NO shows the existence of different conformers in hemoglobin (Maxwell & Caughey, 1976); it will be interesting to perform a similar study on Mb and its mutants to establish if there is a connection with the observed kinetics.

Because of the extraordinary sensitivity of NO rebinding rates resulting from the wide variety of mutants of human myoglobin considered here, we conclude that if changes in the kinetics occur on a tens of picoseconds timescale, then either there is fast communication between protein residues over quite long distances or there are subtle differences in protein structure that exert great control over the reaction dynamics.

We thank B. Bohn and Dr M. C. Marden for help in preparation of the samples. Parts of this work were supported by a grant from National Institutes of Health (GM-27738) and by grants from INSERM, ENSTA and Le Ministère de la Recherche et de l'Espace.

References

Adachi, S., Sunohara, N., Ishimori, K. & Morishima, I. (1992). Structure and ligand binding properties of leucine 29(B10). *J. Biol. Chem.* **267**, 12614–12621.

Austin, R. H., Beeson, K. W., Eisenstein, L., Frauenfelder, H. & Gunsalus, I. C. (1975). Dynamics of ligand binding to myoglobin. *Biochemistry*, **14**, 5355–5373.

Balasubramanian, S., Lambright, D. G. & Boxer, S. G. (1993*a*). Perturbations of the distal heme pocket in human myoglobin mutants probed by infrared spectroscopy of bound carbon monoxide: correlation with ligand binding kinetics. *Proc. Nat. Acad. Sci., U.S.A.* **90**, 4718–4722.

Balasubramanian, S., Lambright, D. G., Marden, M. C. & Boxer, S. G. (1993*b*). Carbon monoxide recombination to human myoglobin mutants in glycerol-water solutions. *Biochemistry* **32**, 2202–2212.

Carver, T. E., Olson, J. S., Smerdon, S. J., Krzywda, S., Wilkinson, A. J., Gibson, Q. H., Blackmore, R. S., Ropp, J. D. & Sligar, S. G. (1991). Contributions of residue 45(CD3) and heme-6-propionate to the bimolecular and geminate recombination reactions of myoglobin. *Biochemistry*, **30**, 4697–4705.

Case, P. A. & Karplus, M. (1979). Dynamics of ligand binding to heme proteins. *J. Mol. Biol.* **132**, 343–368.

Cornelius, P. A., Hochstrasser, R. M. & Steele, W. A. (1983). Ultrafast relaxation in picosecond photolysis of nitrosylmyoglobin. *J. Mol. Biol.* **163**, 119–128.

Elber, R. & Karplus, M. (1990). CO diffusion in myoglobin. *J. Amer. Chem. Soc.* **112**, 9161–9175.

Findsen, E. W., Friedman, J. M., Ondrias, M. R. & Simon, S. R. (1985). Picosecond time-resolved resonance Raman studies of hemoglobin: implications for reactivity. *Science*, **229**, 661–665.

Genberg, L., Richard, L., McLendon, G. & Miller, R. J. D. (1991). Direct observation of global protein motion in hemoglobin and myoglobin in picosecond time scales. *Science*, **251**, 1051–1054.

Gibson, Q. H., Olson, J. S., McKinnie, R. E. & Rohlfs, R. J. (1986). A kinetic description of ligand binding to sperm whale myoglobin. *J. Biol. Chem.* **261**, 10228–10239.

Hubbard, S. R., Hendrickson, W. A., Lambright, D. G. & Boxer, S. G. (1990). X-ray crystal structure of a recombinant human myoglobin mutant. *J. Mol. Biol.* **213**, 215–218.

Ikeda-Saito, M., Dou, Y., Yonetani, T., Olson, J. S., Li, T., Regan, R. & Gibson, Q. H. (1993). Ligand diffusion in the distal heme pocket of myoglobin: a primary determinant of geminate rebinding. *J. Biol. Chem.* **268**, 6855–6857.

Jaynes, E. T. (1986). *Maximum Entropy and Bayesian Methods in Applied Statistics* (Justice, J. H., ed.), pp. 26–58, Cambridge, Cambridge University Press.

Jongeward, K. A., Magde, D., Taube, D. J., Marsters, J. C., Traylor, T. G. & Sharma, V. S. (1988). Picosecond and nanosecond geminate recombination of myoglobin with carbon monoxide, oxygen, nitric oxide and isocyanides. *J. Amer. Chem. Soc.* **110**, 380–387.

Jongeward, K. A., Marsters, J. C. & Magde, D. (1986). Ultrafast studies of nitrosylmyoglobin. In *Ultrafast Phenomena V* (Fleming, G. R. & Siegman, A., eds), pp. 427–429, Springer, Berlin.

Kendrew, J. C., Dickerson, R. E., Strandberg, B. E., Hart, R. G., Davies, D. R., Phillips, D. C. & Shore, V. C. (1960). Structure of myoglobin. *Nature (London)*, **185**, 422–427.

Kuriyan, J., Wilz, S., Karplus, M. & Petsko, G. A. (1986). X-ray structure and refinement of carbon-monoxy (iron-II) myoglobin at 1·5 Å resolution. *J. Mol. Biol.* **192**, 133–154.

Lambright, D. G., Balasubramanian, S. & Boxer, S. G. (1989). Ligand and proton exchange dynamics in recombinant human myoglobin mutants. *J. Mol. Biol.* **207**, 289–299.

Lambright, D. G., Balasubramanian, S. & Boxer, S. G. (1991). Protein relaxation dynamics in human myoglobin. *Chem. Phys.* **158**, 249–260.

Lambright, D. G., Balasubramanian, S. & Boxer, S. G. (1993). Dynamics of protein relaxation in site-specific mutants of human myoglobin. *Biochemistry*, **32**, 10116–10124.

Lecomte, J. T. J. & LaMar, G. N. (1985). Proton NMR study of labile proton exchange in the heme cavity and a probe for the potential ligand entry channel in myoglobin. *Biochemistry*, **24**, 7388–7395.

Li, H., Elber, R. & Straub, J. E. (1993). Molecular dynamics simulation of NO recombination to myoglobin. *J. Biol. Chem.* **268**, 5711–5718.

Livesey, A. K. & Brochon, J. C. (1987). Analyzing the distribution of decay constants in pulse fluorimetry using the maximum entropy method. *Biophys. J.* **52**, 693–706.

Maxwell, J. C. & Caughey, W. S. (1976). An infrared study of nitric oxide binding to hemoglobin B and hemoglobin A. *Biochemistry*, **15**, 388–396.

Petrich, J. W., Lambry, J. C., Kuczera, K., Karplus, M., Poyart, C. & Martin, J. L. (1991). Ligand binding and protein relaxation in heme proteins: a room temperature analysis of nitric oxide geminate recombination. *Biochemistry*, **30**, 3975–3987.

Petrich, J. W., Martin, J. L., Houde, D., Poyart, C. & Orszag, A. (1987). Time-resolved resonance Raman spectroscopy with subpicosecond resolution: vibrational cooling and delocalization of strain energy in photodissociated (carbonmonoxy) hemoglobin. *Biochemistry*, **26**, 7914–7923.

Petrich, J. W., Poyart, C. & Martin, J. L. (1988). Photophysics and reactivity of heme proteins: a femtosecond absorption study of hemoglobin, myoglobin and protoheme. *Biochemistry*, **27**, 4049–4060.

Press, W. H., Flannery, B. P., Teukolsky, S. A. & Vetterling, W. T. (1989). *Numerical Recipes*, Cambridge University Press.

Ringe, D., Petsko, G. A., Kerr, D. & Ortiz de Montellano, P. R. (1984). Reaction of myoglobin with phenylhydrazine: a molecular doorstop. *Biochemistry*, **23**, 2–4.

Skilling, J. (1988). *Maximum Entropy and Bayesian Methods*, Kluwer, Dordrecht.

Skilling, J. & Gull, S. F. (1985). Algorithms and applications. In *Maximum Entropy Methods in Inverse Problems* (Smith, C. R. & Grandy, W. T., eds), pp. 487–542, D. Reidel, Dordrecht.

Smerdon, S. J., Dodson, G. G., Wilkinson, A. J., Gibson, Q. H. & Blackmore, R. S. (1991). Distal pocket polarity in ligand binding to myoglobin: structural and functional characterization of a threonine 68 (E11) mutant. *Biochemistry*, **30**, 6252–6260.

Snyder, S. H. & Bredt, D. S. (1992). Biological roles of nitric oxide. *Sci. Amer.* **May**, 68–77.

Tian, W. D., Sage, J. T., Srajer, V. & Champion, P. M. (1992). Relaxation dynamics of myoglobin in solution. *Phys. Rev. Lett.* **68**, 408–411.

Traylor, T. G. & Sharma, V. S. (1992). Why NO? *Biochemistry*, **31**, 2847–2849.

Varadarajan, R., Lambright, D. G. & Boxer, S. G. (1989). Electrostatic interactions in wild-type and mutant recombinant human myoglobins. *Biochemistry*, **28**, 3771–3781.

Xie, X. & Simon, J. D. (1991). Protein conformational relaxation following photodissociation of carbon monoxide from carbonmonoxymyoglobin: picosecond circular dichroism and absorption studies. *Biochemistry*, **30**, 3682–3692.

Edited by A. R. Fersht

(Received 18 November 1993; accepted 27 January 1994)